ICOLD Symposium on Sustainable Development of Dams and River Basins, 24th - 27th February, 2021, New Delhi

BREACH ANALYSIS OF EMBANKMENT DAMS USING SOFT COMPUTING TECHNIQUES

DEEPAK KR. VERMA
UIET, M. D. University, Rohtak, Haryana, India

BALDEV SETIA AND V.K. ARORA
National Institute of Technology, Kurukshetra, India

ABSTRACT

Embankment dams are beneficial to people since early days of civilization. In spite of many benefits, the failure of a dam causes loss of lives and property. In case of embankment dams, the overtopping failure is the common cause of embankment failure. To understand the breaching process, it is essential to determine breach parameters (breach width, breach depth, peak outflow) experimentally. Present study describes different tests conducted in four different flumes. For developing emergency action plans (EAP), it is essential to determine and analyze different breach parameters. The temporal variations of breaching process were observed and described in different phases. Soft computing techniques i.e. artificial neural network (ANN) and multi-linear-regression (MLR) are used to determine peak outflow from embankment breach data. For the assessment of embankment breaching, accurate prediction of peak outflow from breached embankments is important. In the present study, an efficient model was developed to predict peak outflow by using ANN and MLR. Historical dam failure data was also used to train and evaluate the applicability of these models. This study indicated that the breach phenomenon is strongly dependent upon the cohesive forces of the fill material and hydraulic characteristics of flow. Also, the soil characteristics of fill material in-fluence the rate of breaching of embankment dams. The developed model probably can be used as predictive tool for estimation of peak outflow of embankment dams in case of overtopping of failure.

1. INTRODUCTION AND LITERATURE

Embankment dams are built since early days of human civilization and are beneficial to people throughout the world. They are used for flood control, irrigation, water supply, navigation etc. In spite of many benefits to the society, these dams are highly associated with some trigger mechanisms like overtopping, seepage, landslides etc which involve high risk to lives and properties. The studies (Foster and Fell, 2001) described that overtopping is the major cause of embankment failure. Owing to failure of dam, population centers near the dam suffer huge loss of lives and damage of property. Therefore it is essential to analyze the breaching of embankments to reduce the causalities by developing early warning systems. USBR (1988) grouped the breach analysis methods into four categories and critically described by Singh (1996). Breach modeling as parametric models, predictor equations, physically based methods and comparative analysis adopted by many researchers in the direction of breach analysis of embankments. Using parametric breach models and predictor equations, the different breach parameters like breach width, breach depth, peak outflow and time to failure could be determined using statistically derived equations (Walder and O'Connor (1997), Xu and Zhang (2009). These models were highly influenced by the accuracy of data available. Physical models based on some assumptions to simplify the breaching process (Fread 1988, Wu 2013) and detailed physical models are quite complicated and costly to use (Wahl et al. 2008; Wu et al. 2011). Breach modeling critically reviewed by Wahl (2007) and Wu (2011) and found different uncertainties in the prediction of breach parameters. These models described the routing tasks efficiently but could not describe the development of breach and temporal variations of different breach parameters which are essential to understand the breach behavior during overtopping. Wu (2011) reviewed different breach modeling used by the researchers and concluded that the effect of fill material was considered only in a few models. Further it was concluded that to improve the knowledge regarding breaching process, it is necessary to conduct small or large scale experimental studies. Wu (2011) tabulated different laboratory experiments and field case studies conducted by many investigators in the past few decades. These laboratory and field studies were based on erosion mechanics and gave a better idea regarding breach growth. The breach parameters can also be determined in the laboratory by varying the dimensions of embankment models, composition of fill material and hydraulic conditions. Recently experimental studies were

carried out by a few researchers (Zhu et al, 2011; Sahu et al, 2013; Verma et al, 2014; Jhao, 2014; Verma et al 2017) to understand the breaching of embankments and observed the different breach parameters.

From the above review of literature, it is clear that none of the approaches is fully equipped in itself to provide a complete solution to the prediction of breach parameters of width, intensity, time etc. Therefore, it becomes essential to conduct small scale or large scale tests which help to address many of the shortcomings identified in literature. Further there should be correlation between laboratory tests and the realistic dam failures. In order to get more facts in this direction present paper describes the laboratory investigations to understand the embankment breaching due to overtopping.

2. EXPERIMENTAL SETUP AND PROCEDURE

With the major objective of studying the breach mechanism, a study was planned and a total 224 experiments were conducted in four different flumes under different conditions to understand and analyze the breach behavior during and after the overtopping of embankments. The experiments were carried out in flume A, B and C, the Hydraulics Laboratories of Civil Engineering Department of the National Institute of Technology (NIT), Kurukshetra and in flume D, the Hydraulics Research Laboratory of Civil Engineering Department at Maharishi Markandeshwar (Deemed to be University) (MMU), Mullana, Ambala (India) as shown in Figures 1-4.

Figure 1 (a) : Pictorial View

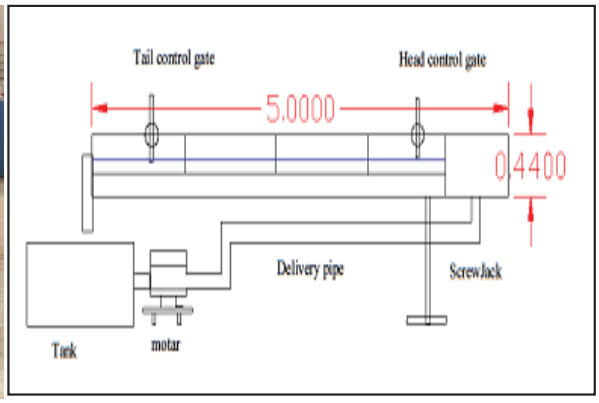

Figure 1 (b) : Line Diagram

Figure 1 : Pictorial View and Line Diagram of Small Recirculating Flume A (3.10m Long, 0.25m Wide, 0.30m Deep); NIT, Kurukshetra)

Figure 2 (a) : Pictorial View

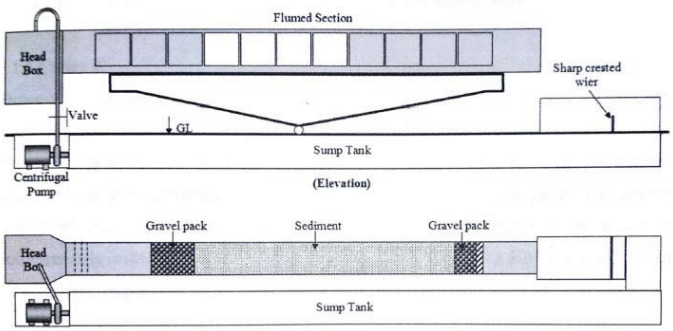

Figure 2 (b): Line Diagram

Figure 2 : Pictorial View and Line Diagram of Tilting Bed Flume B (12m Long, 0.40m Wide, 0.50m Deep; NIT, Kurukshetra)

Figure 3 (a) : Pictorial View

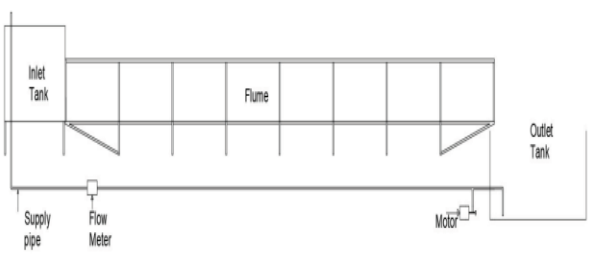

Figure 3 (b) : Line Diagram

Figure 3 : Pictorial View and Line Diagram of Recirculating Flume C (10m Long, 0.60m Wide, 0.60m Deep; NIT, Kurukshetra)

Figure 4(a) : Pictorial View

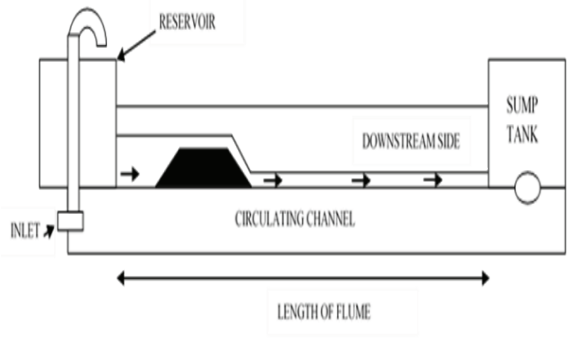

Figure 4 (b) : Line Diagram

Figure 4 : Pictorial View and Line Diagram of Reciculating Flume D (4.5m Long, 0.60m Wide, 0.60m Deep; MMEC, Mullana)

2.1 Experimental program

The position of the embankment models inside the flume for all tests was same. The coarse and fine grained soils of different proportion were utilized as fill material. The embankment material was mixed at optimum moisture content corresponding to maximum dry density and was placed in layers of 8 cm each. These layers were compacted with a hand operated compaction roller (Figure 5). To reduce seepage, a layer of pure clay was placed on upstream side of embankment. After construction, the model was left as such in this position for 24-48 hours. This would allow the material in the model to stabilize itself. After a suitable lay-off water was filled on upstream side of the dam up to the pre-determined level leaving a free board of 4 cm. After filling the water on upstream side of embankment, it was retained about 20 hours for homogeneous saturation of embankment.

Figure 5 : Hand Operated Compaction Rollers

During the process of overtopping, the temporal variation of breach width and depth were observed with the help of pointer gauge, staff gauge and stop watch. The different breach characteristics as breach initiation time, breach formation time and time to breach were noted down for each experiment. These breach characteristics were essential to describe the correlation between soil erodibility and geotechnical parameters. The whole process was videotaped with a high speed digital video camera (Fastec Imaging Inline Gigabyte Ethernet Camera) as shown in Figure 6 and instant photographs were taken with digital cameras.

Figure 6 . Fastec Imaging Inline Gigabyte Ethernet Camera

2.2 Analysis of breach mechanism

By conducting different experiments in the laboratory, it was observed that progressive surface erosion oc-curs for non-cohesive soil (Figure 7) and for cohesive embankment; headcut erosion occurs (Figure 8). For non-cohesive soils, the sand grains act as individual particles and once the velocity of flow is higher than the threshold value of initiation of sands; the particles immediately start to move. In the possibility of breaching of the embankment, the flow velocities become very high and the embankment failure is instantaneous. However, in the case of cohesive soils, the soils because of strong inter-particle bondage do not move with the flow. The soil acts as a lump and accordingly, the failure is gradual. But in both the cases, breach initiation starts at the toe of the downstream side. The cohesive proportion in the sand-silt-clay mixtures slowed down the erosion process. Laboratory experimentation shows that the erosion process occurs due to the detachment of embankment material by overtopping flow during breaching of embankment.

Figure 7 : Surface erosion of non-cohesive soil

Figure 8 : Headcut erosion of cohesive soil

The results of the experimental observations have been analyzed and discussed under the following subheadings: Evolution of breach and Embankment profile.

2.2.1 *Evolution of breach*

As the high flood level (HFL) becomes slightly higher the level of the top of the crest, the sheet of water moves to the downstream from over the dam. The dam is, thus, overtopped. The initial energy of the overtopping sheet of water for a few seconds is resisted by the compacted surface of the dam, after which it begins to erode at the downstream face of the crest. Researchers in the past have described the breach phenomenon in different phases. Accordingly, here it is being described in three phases. The breach growth for cohesive and non-cohesive embankments is described under 3 phases with some exceptions. On the basis of observations of different tests, these three phases are explained as

Phase of breach initiation : Both the categories of fuse plugs had same fill material in the analogous models. Accordingly they exhibited similarities in the initiation of erosion. For models with predominantly non-cohesive material, the first signs of erosion were observed on the surface of the downstream face of the filling along the path of first stream of overtopping water (Figure 7). The material on the surface was not able to resist the erosion and in a matter of about 10 sec the water had developed a narrow channel.

However, in the case of model with cohesive material, the overtopping water failed to make any distinct mark on the crest or the downstream face for a considerable duration. The first visible sign of erosion commenced at the downstream toe of the fill material (Figure 8) and progressed upward. It was very clear that whereas for the non-cohesive material it started from top to bottom, it started from bottom towards up in the predominantly cohesive material. However for the same fill material there was no basic difference in the two categories of fuse plugs in the initiation of erosion. The same observations match with the observations of Walder and Godt (2015) .

Phase of breach progression : In this phase, the breach progresses due to continuous overtopping. The progression for pre dominantly non-cohesive fill material was interrupted due to caving in of sediments. Also different irregular gradients on downstream face were observed which accelerated towards the upward direction. For cohesive fill material, the step migration of erosion occurred after 5-15 minutes from the phase of breach initiation. It was due to detachment of sediment in lumps with increased magnitude which caused the widening of the breach. These experiments are useful to understand the erosion mechanisms of breach under cohesive and non-cohesive fill material because of the confinement of the side walls, the process, at best presents a 2-D breach analogy. The experiments conducted by Schmocker and Hager [25] support these results. According to these authors, the morphodynamics of 2-D experiment, in which water spills over the entire embankment, were different as the water surface would be nearly parallel to the bed surface.

Phase of time to breach: Due to continuous outflow, the headcut migrates along the entire length of downstream side. It progressively increased towards upstream and downward, with increasing discharge. Also, the breach channel widens as

the sediment from the banks are passages by the flow of water and heavy sediments are progressively eroded. With the abrupt cutting of banks, the lengthening of breach crest may be dislocated. For cohesive soil, the instead of progressive erosion as in case of non-cohesive soil, headcutting was observed which advances longitudinally

2.2.2 *Embankment profile*

The results of above mentioned tests are taken for describing water surface profile through channel. The temporal variation of breach for cohesive and non-cohesive soil was plotted w.r.t. embankment depth as shown in Figures 9 and 10. It was also observed that it is essential to control compaction during the construction of earthfill model since it affects the rate of erosion. It was concluded that there is gradual erosion for non-cohesive soil and step erosion for cohesive soil.

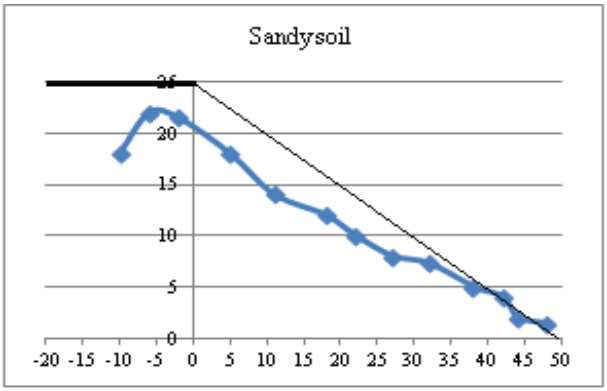

Figure 9 : Progress of breach for sandy soil Duration of test 4 mins

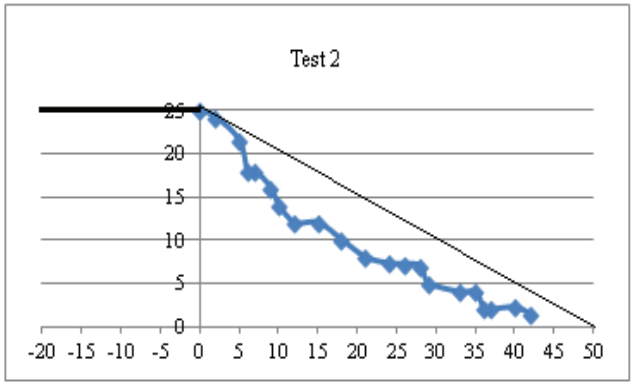

Figure 10 : Progress of breach for cohesive soil Duration of test 29 mins

3. ARTIFICIAL NEURAL NETWORK (ANN) FOR PEAK OUTFLOW

Different regression techniques are used to analyze the correlation among different breach parameters. Present experimental data set is used to obtain optimized relations using Artificial Neural Network (ANN) and Random Forest (RF) techniques. On the basis of optimized correlations, the equations have been developed using Multi-Linear-Regression (MLR). The specific characteristics of the present data are mentioned in Table 1.

Table 1 : Specific Characteristics of Data

S. No.	Variables		Minimum	Maximum	Mean	SD
1	q (cm^3/sec/cm)	Discharge intensity	49.1	300	136.6	94.069
2	H_d (cm)	Dam height	10	35	23.57143	8.131
3	W (cm)	Crest width of embankment	5	25	14.64286	5.51
4	Z (tan θ)	Slope of downstream dam face	0.5	1	0.727857	0.185
5	D_{50} (mm)	Mean particle size	0.005	0.6	0.232464	0.215
6	B_0 (sec)	Breach initiation time	2	135	22.85268	27.453
7	d_w(cm)	Depth of water at time of breach	2.4	33.2	19.60313	8.001
8	V_w (cm_3)	Volume of water at time of breach	9300	1096320	424569.5	295837.5
9	Q_p (cm^3/sec)	Peak outflow	84	58321	13012.24	11146.2
10	t_f(sec)	Time to failure	29	345	102.1116	55.411
11	B_{bavg} (cm)	Average breach width	18	56.5	38.74107	11.28
12	h_b (cm)	Breach height	2	33	19.16964	7.963

3.1.1 Optimized Relation Using Artificial Neural Network

Experimental results observed in the present experimental study were analyzed using ANN regression analysis. The procedure of analysis comprises the following steps:

(a) Sensitivity Analysis

(b) Selection of optimized parameters

(c) Optimized relation for peak outflow

(d) Comparison of actual and predicted values for peak outflow

(a) Sensitivity Analysis : In sensitivity analysis, the data set is divided in two sections. In compliance with the requirement of data division; the data set of present study has been split into 70% for training and 30% for testing. For regression using ANN, the specific values of user-defined functions, based on previous available research works, was used in the present study. The values of these functions for optimal results are: Learning Rate = 0.2; Momentum = 0.1; Training Time = 500. As described above, there are a total of 8 variables used in the present study.

Selection of Neural Network : Using the above constraints, the data was used for regression and results were obtained in the form of Coefficient of Correlation (CC) and Root Mean Squared Error (RMSE) corresponding to each value of neural network. The results were analyzed on the basis of performance measurement for both training and testing results and selected number of neural network was 18 as shown in Figure 11.

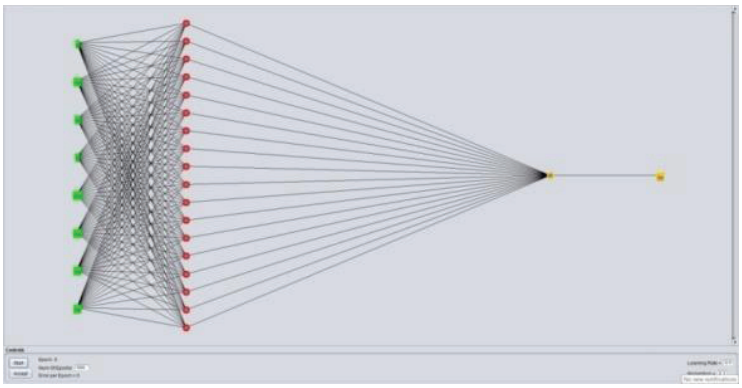

Figure 11 : Pictorial Representation of Selected Neural Network for Peak Outflow

The values of the performance measurement for both training and testing data set corresponding to optimum neural network of 18 are mentioned in Table 2.

Table 2 : Values of CC and RMSE for Selected Neural Network (HL = 18) for Q_p

HL	Training Data Set		Testing Data Set	
18	Correlation coefficient	0.9874	Correlation coefficient	0.987
	Mean absolute error	1203.4669	Mean absolute error	1437.8792
	Root mean squared error	1757.8765	Root mean squared error	1880.515
	Relative absolute error	14.881%	Relative absolute error	18.2347%
	Root relative squared error	15.9043%	Root relative squared error	16.6727%
	Total Number of Instances	153	Total Number of Instances	71

(b) Selection of optimized parameters : By obtaining the appropriate hidden layer, the deviation of different variables for different combinations was obtained. The variables were optimized by analyzing their deviations in terms of performance measurement parameters. The most important parameters were obtained on the basis of present study data, previous studies in addition to performance measurement. The optimized parameters are defined in the relation as:

$$\text{Model} : Q_p = \phi(D_{50}, d_w, V_w) \qquad \text{….. Eq. 1}$$

Corresponding optimum values for CC and RMSE for the testing were 0.987 and 1880 respectively.

(c) Optimized relation for peak outflow : To obtain an optimized relation for these parameters, the same procedure was repeated and analyzed for selecting the hidden layer. On the basis of performance measurements of training and testing data set, the neural network was selected. For optimized hidden layer, different combinations were made using different parameters. To obtain an optimal relation for peak outflow, CC and RMSE of different combinations were analyzed. It was determined that the input variables that correlate with the peak outflow, Q_p are d_w, V_w and D_{50}. For this relation, the predicted values of Q_p were obtained and the graphs were plotted for the predicted and actual values of training and testing data.

(d) Comparison of actual and predicted values for peak outflow: Figure 12 is showing the comparison of actual and predicted values of peak outflow for training and testing data of present study. It was observed that for Training data set, the predicted values correlate with the actual values as shown in Figure 12 (a). Similarly for testing data, the results of predicted outflow were obtained and plotted as shown in Figure 12 (b). It was observed that the predicted value follows almost the same trend as for Training data set. Also the predicted values are slightly overestimated for most of the data points.

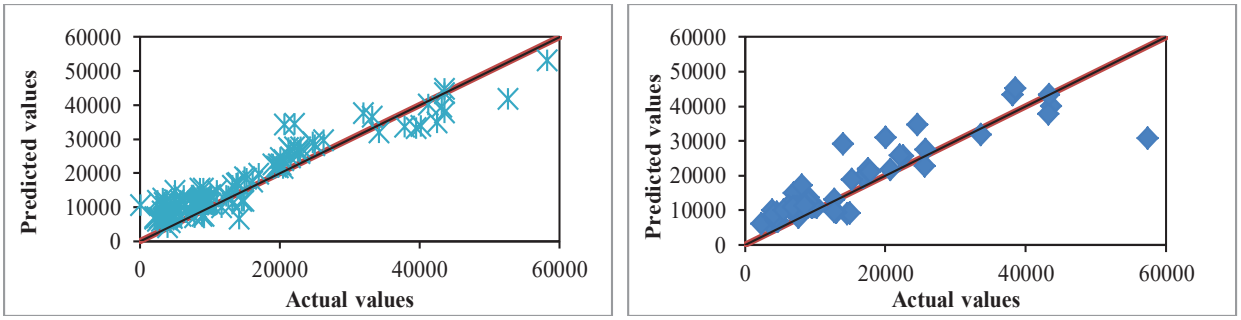

Training data set Testing Data

Figure 12 (b) : Comparison of Actual and Predicted Values for Peak Outflow, ANN

To observe the variation of actual and predicted values, peak outflow values of all embankment models were used for training and testing data. The results have been plotted between embankment models on X-axis and peak outflow on Y-axis. Two curves corresponding to actual and predicted values were drawn as shown in Figure 13 (a) and 13 (b). From Figure 13 (a), it was observed that actual values agree with predicted values of peak outflow. The figure also indicates that actual and predicted values follow a common trend for Training data set. Similarly the results of testing data was observed and plotted for different embankment models as shown in Figure 13(b).

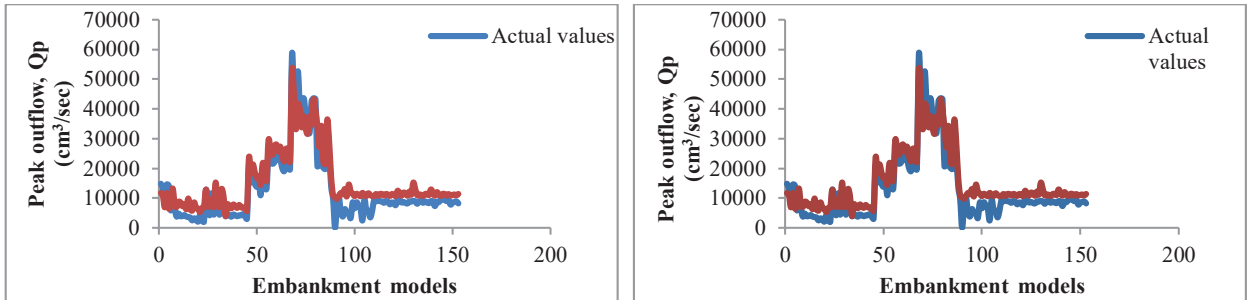

(a) Training Data Set (b) Testing Data Set

Figure13 : Variation of Actual and Predicted Values for Embankment Models, ANN

3.1.2 Multi-Linear-Regression

Further the optimized parameters, selected using ANN and RF for peak outflow,were used to develop a relation. The Multi-Linear-Regression (MLR) is used to correlate different significant parameters to predict peak outflow. A relation was proposed on the basis of present experimental data which is as follows:

Model $Q_p = 2.6D_{500}^{.14}V_w^{0.87}{}_{dw}^{-0.}8$ ….. Eq. 2

A graph between actual and predicted values was obtained as shown in Figure 14 (a). It was observed that present study data points lie equidistant from zero error line. Figure 14 (b) indicates the residuals of actual and predicted outflow for embankment models. It indicates that the residuals lie in a specific range of -6000 to +2000 for most of the embankment models.

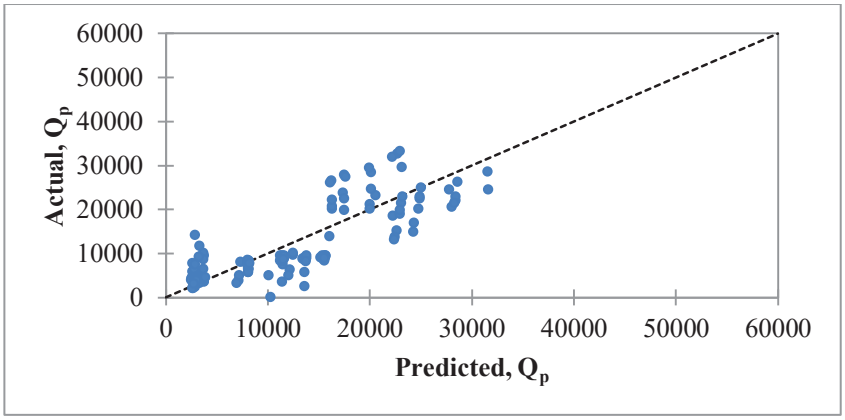

Figure 14 (a) : Comparison of Actual and Predicted Values for Peak Outflow (MLR)

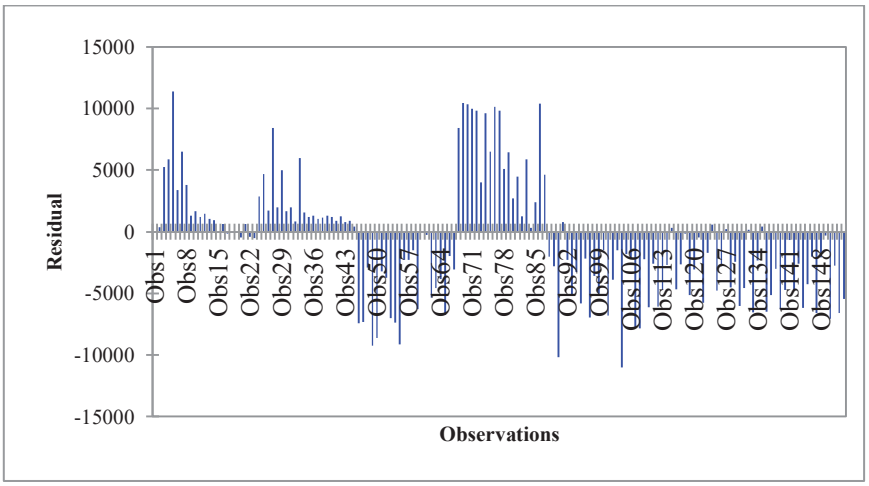

Figure 14 (b) : Residuals of Actual and Predicted Values for Embankment Models (MLR)

3.1.3 Analysis using present data and other laboratory data

Extending the analysis further, the present study data was combined with other experimental data (Chinnarasri et al., 2004). The ANN technique was used for this combined data. The performance measurements were obtained for the same relation as mentioned in Equation 2. The data points were plotted for actual and predicted values of peak outflow (Figure 15a). It was observed that all the data points form a cluster except two points. It indicates that the optimized relation obtained by ANN for present data closely agrees with other laboratory data. The same observations were found by plotting the variation of actual and predicted values as shown in Figure 15 (b).

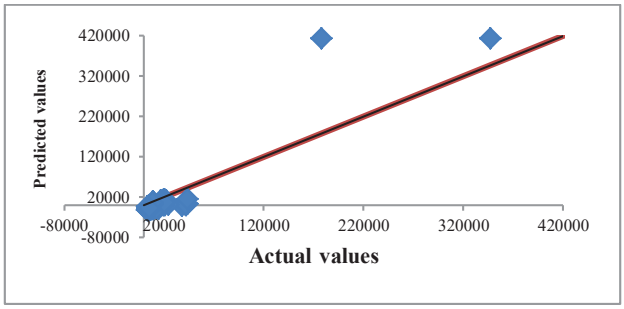

(a) Testing Data Set

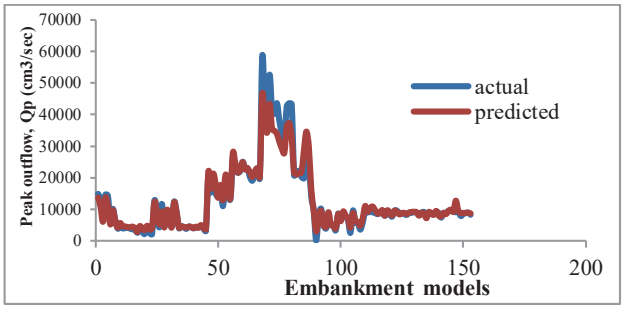

(b) Testing Data Set

Figure 15 : Variation of Actual and Predicted Values of Other Laboratory Data with Model, ANN

4. SUMMARY AND CONCLUSIONS

Experiments on breaching of embankments were conducted by varying dam length, discharge intensities and geotechnical parameters. From the detailed analysis of the experimental results of embankment breaching and the data of previous researchers it could be inferred:

(i) Overtopping of an earthen embankment marks the beginning of the breach and breaching process.

(ii) After the overtopping of embankment, breaching process starts with initial erosion of the embankment surface that proceeds towards the toe. After surface erosion at toe, the headcut erosion develops in a zigzag migration possibly due to non-homogeneous characteristics of the embankment material. The observation matches with the hypothesis that was strongly supported by Hanson et al. (2011).

(iii) Headcut migration advances towards the embankment crest and simultaneously the erosion triggers in lateral direction to widen the breach.

(iv) Surface erosion, headcut erosion and lateral erosion comprise the erosion process of embankment breaching.

(v) For non-cohesive soil, the progressive erosion occurs and with the passage of time, the breach discharge increases abruptly and decreases as the breach widens.

(vi) In case of cohesive soil, headcut erosion occurs due to detachment of soil mass. On the other hand, surface erosion takes place for non-cohesive soil. The cohesiveness of soil directly influence the duration of breaching of earthen dams.

(vii) During the breaching of embankment model, the erosion is a three dimensional process and the migration of erosion is associated with lateral widening. Rate of widening depends on the rate of headcut migration.

(viii) From different breach parameters of present study, the optimized significant parameters were obtained using ANN and RF techniques. These parameters are used for Multi Linear Regression (MLR) and three equations were developed for predicting peak outflow (Q_p), time to failure (t_f) and average breach width (B_{bavg}) which are as follows:

$$\text{Model : } Q_p = 2.6D_{50}^{0.14}V_w^{0.87}d_w^{-0.8}$$

The model compared with the other experimental data of Chinnarsari et al. (2004). The predicted values using Model 1 yield closer results.

5. SCOPE FOR FURTHER STUDIES

It is necessary to conduct large scale experiments to understand the breach mechanism and relate different breach parameters. Historical data would be obtained from photographs, eyewitness reports, discharge measurement etc. However, it is very difficult and dangerous to obtain the data from the field study. A possible way to reduce damage of embankment is to relate dependent variable breach width (B_b) with independent variable dam height (H_d). And further correlate time to breach (t_f) with average breach width (B_{bavg}). The laboratory should be further correlated with the sediment transport studies. Since both the subjects are of empirical nature, only laboratory experimental work can help in establishing better and reliable results. The scale and range of the flumes and soil compositions should be increased.

6. REFERENCES

Chinnarasri, C., Jirakitlerd, S., and Wongwises, S. 2004. Embankment dam breach and its outflow character-istics. Civ. Eng. Environ. Syst., 21(4), 247-264.

Foster, M. and Fell, R. 2001. Assessing embankment dams, filters which do not satisfy design criteria, Journal of Geotechnical and Geo-environmental Engineering, ASCE, 127 (4)

Hanson, G. J., Temple, D. M., Hunt, S. L., and Tejral, R. D. 2011. Development and characterization of soil material parameters for embankment breach. Appl. Eng. Agric., 27(4), 587-595.

Jhao, G. 2014, Breach growth in cohesive embankments due to overtopping, Ph.D. thesis, Delft University of Technology, ISBN: 97890-6562-3942 (online).

O'Connor, J. E. and Beebee, R. A., 2009. Floods from natural rock-material dams, in Mega flooding on Earth and Mars, Cambridge Univ. Press, Cambridge, England: 128–171.

Sahu, K.C., Das P.K. and Gangadharaiah T. 2013, Breach flow hydrograph due to wash out of Fuse plug in an Earthen Dam, World Applied Sciences Journal, 28 (5): 711-717.

Singh, V.P. 1996, Dam Breach modeling Technology, Kluwer Academic Publisher.

U.S. Bureau of Reclamation 1988, Downstream Hazard Classification Guidelines, ACER Technical Memo-randum No. 11, Assistant Commissioner-Engineering and Research, Denver, Colorado, 57.

Verma, D. Setia, B. and Arora, V.K. 2014. Mechanism of embankment dam breach, Published in Proceedings of the International Conference on Fluvial Hydraulics, EPFL, Switzerland, River Flow 2014, Retrieved from www.scopus.com.

Verma, D. Setia, B. and Arora, V.K. 2017. Experimental study of breaching of an earthen dam using a fuse plug model, International Journal of Engineering, 30 (4), pp. 479-485.

Walder, J. S., and O'Connor, J. E. 1997, Methods for predicting peak discharge of floods caused by failure of natural and constructed earth dams. Water Resources Research, 33(10), 2337–2348.

Wahl, T.L. 2007, Uncertainty of Predictions of Embankment dam breach parameters, Journal of Hydraulic Engineering, 130 (5): 389-397.

Wahl, T. L. 2008, Development of next-generation embankment dam breach models, U.S. Society on Dams Annual Meeting and Conference, Portland, 767–779.

Walder, J. and Godt, J.W. 2015, Controls on the flood hydrograph and breach geometry during overtopping of non-cohesive earthen dams, Water Resources Research, DOI: 10.1002/2014WR016620.

Wu, W. 2011, Earthen Embankment Breaching, Journal of Hydraulic Engineering, DOI: 10.1061/ (ASCE) hy.1943-7900.0000498: 1549-1564.

Wu, W. 2013, Simplified Physically Based Model of Earthen Embankment Breaching, Journal of Hydraulic Engineering, ASCE, 139 (8): 837-851.

Xu, Y. and Zhang, L.M. 2009, Breaching parameters for earth and rock fill dams, Journal of Geotechnical and Geo-environmental Engineering, 135(12): 1957-1969.

Zhu Y. H., Visser P. J., Vrijling J. K. and Wang G. Q. 2011, Experimental investigation on breaching of em-bankments, Sci China Tech Sci, 54: 148−155.